

# Site- and enantioselective allylic and propargylic C-H oxidation enabled by copper-based biomimetic catalysis

Honggang Zhang,<sup>1</sup>† Yibo Zhou,<sup>1</sup>† Tulong Yang,<sup>2</sup>† Jingui Wu,<sup>1</sup> Pinhong Chen,<sup>1</sup> Zhenyang Lin,<sup>2\*</sup>  
Guosheng Liu<sup>1\*</sup>

<sup>1</sup>New Cornerstone Science Laboratory, State Key Laboratory of Organometallic Chemistry and Shanghai Hongkong Joint Laboratory in Chemical Synthesis, Shanghai Institute of Organic Chemistry, University of Chinese Academy of Sciences, Chinese Academy of Sciences, 345 Lingling Road, Shanghai, China, 200032.

<sup>2</sup>Department of Chemistry, The Hong Kong University of Science and Technology, Clear Water Bay, Kowloon, Hong Kong, China.

\* Correspondence to: [gliu@mail.sioc.ac.cn](mailto:gliu@mail.sioc.ac.cn) (G.L.); [chzlin@ust.hk](mailto:chzlin@ust.hk) (Z.L.)

† These authors contributed equally.

**Methods for direct, enantioselective oxidation of C(*sp*<sup>3</sup>)-H bonds in organic molecules will revolutionize the preparation of chiral alcohols and their derivatives, which are important moieties in natural products, pharmaceuticals and agrochemicals. Enzymatic catalysis, which employs key metal oxides to facilitate efficient hydrogen atom abstraction, has evolved as a highly selective approach for C-H oxidation in biological systems. Despite its effectiveness, reproducing this function and achieving high stereoselectivity in biomimetic catalysts has proven to be a daunting task. Here we present a copper-based mimetic catalytic system that achieves highly efficient asymmetric *sp*<sup>3</sup> C-H oxidation with the C-H substrates as the limiting reagent. An unprecedented Cu(II)-bound *tert*-butoxy radical is responsible for the site-selective C-H bond cleavage, which resembles the active site of copper-based enzymes for C-H oxidation. The developed allylic and propargylic C-H oxidation reactions have been successfully accomplished with good functional group compatibility and exceptionally high site- and enantioselectivity, and this method is applicable for the late-stage oxidation of bioactive compounds.**

Optically pure alcohols are prevalent motifs in natural products and pharmaceuticals, thus tremendous efforts have been made to develop effective methods for their synthesis<sup>1,2</sup>. The  $sp^3$  C-H oxidation has emerged as one of the most powerful and straightforward approaches for accessing alcohols and their derivatives from readily available starting materials<sup>3-10</sup>. However, the asymmetric version of this approach presents significant challenges and remains limited in its scope<sup>11-15</sup>, not to mention that the site- and enantioselective C-H oxidation is a long-standing challenge. To explore the synthetic utility of the methods, regulating both efficiency and enantioselectivity of the reaction with C-H substrates as limiting agents is also important, which has not been addressed so far. In contrast, enzymatic catalysis often exhibits unmatched efficiency and selectivity, particularly concerning the site- and enantioselectivity<sup>16-18</sup>. A core structure of metal oxides is generally involved to facilitate efficient hydrogen atom abstraction, resulting a highly selective approach for C-H oxidation in biological systems. For instance, copper-based enzymes such as LPMO and pMMO demonstrate remarkable abilities to perform efficient and selective  $C(sp^3)$ -H oxidation<sup>19-20</sup>, which relies on Cu-O radical intermediates (Fig. 1A) to accomplish hydrogen atom abstraction (HAA) from strong C-H bonds. This structural motif has inspired many researchers to design various copper-based enzyme models for enzyme mimetic catalysis<sup>18,21</sup>; however, these synthetic systems typically involve Cu-O-Cu clusters that display very limited HAA reactivity. In other words, the development of Cu-based mimetic catalysis still presents a significant and daunting challenge. *To effectively mimic the enzymatic catalysis, especially in terms of site- and enantioselective  $C(sp^3)$ -H oxidation, the designed enzyme mimics must possess two key features: strong HAA abilities and scaffold that possesses similar chiral pockets in enzymes.* We speculated that, if the commonly reported alkoxy radicals (e.g. *tert*-butoxy radical) could bind to active Cu(II) species, the resulting Cu(II)-bound alkoxy radicals (Fig. 1B) would more closely resemble the enzyme active sites. The most crucial aspect of the system design is to prevent the formation of Cu-O-Cu clusters, thereby preserving strong HAA ability of the formed Cu(II)-bound alkoxy radicals. In addition, introducing structurally tunable chiral ligands here provides the

opportunity to build the necessary chiral pocket, thus further improving the functionality of these Cu-based enzyme models. Inspired by asymmetric Kharasch-Sosnovsky (K-S) reaction (Fig. 1C), this concept of Cu(II)-bound alkoxy radicals is here demonstrated in the copper-catalyzed asymmetric oxidation of C(*sp*<sup>3</sup>)-H bonds (Fig. 1D). In this work, an unprecedented monomeric copper(II)-bound *tert*-butoxy radical is established as an effective hydrogen atom acceptor with high HAA reactivity and unique capability for exquisite site-selectivity. With this copper-based catalysis, the C(*sp*<sup>3</sup>)-H oxidation reactions show excellent site- and enantioselectivity and high efficiency with alkenes and alkynes as the limiting reagents. This synthetic strategy provides quick and straightforward access to optically pure alcohols and their derivatives from readily available starting materials, and enables to the late-stage oxidation of natural products and pharmaceuticals with excellent site- and stereoselectivity.

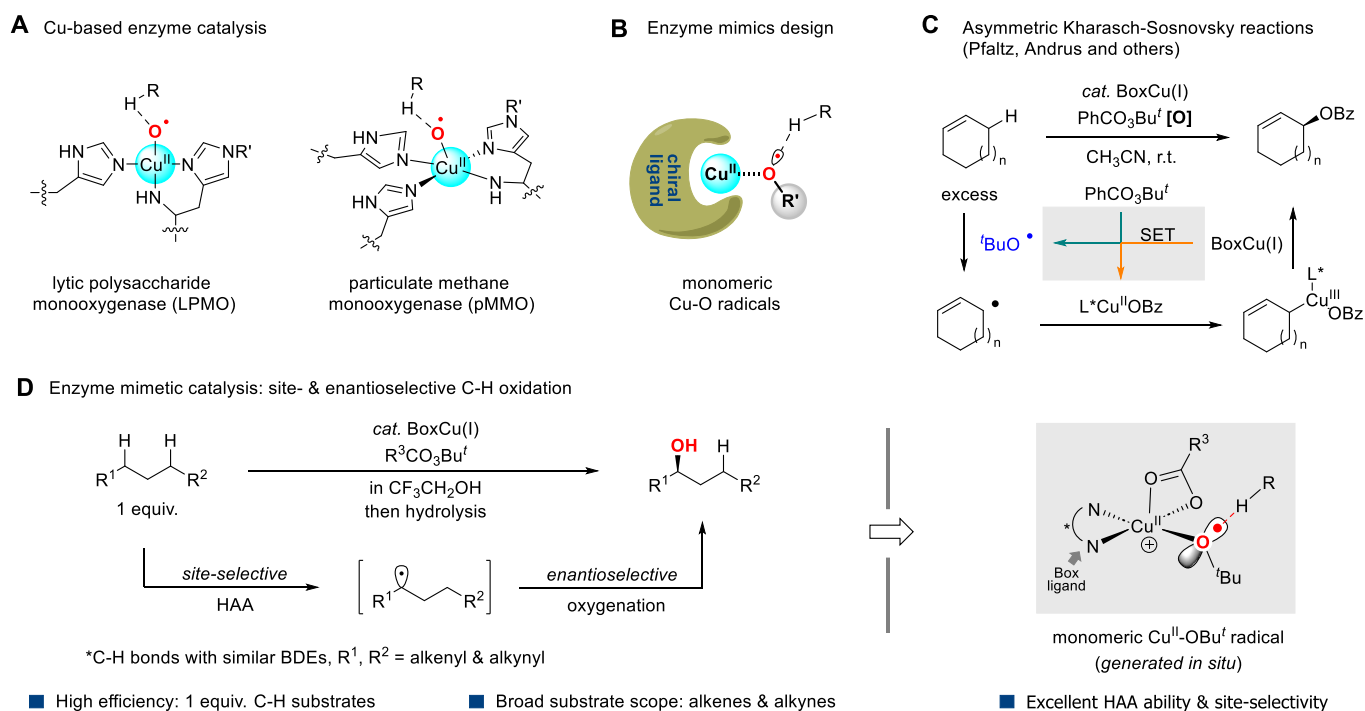


**Fig. 1. Highly selective *sp*<sup>3</sup> C-H oxidation.** **A.** Enzyme catalysis with copper-based enzymes: the structures of active copper oxygen intermediates in LPMO and pMMO. **B.** The concept on the Cu-based enzyme mimics design. **C.** Catalytic *sp*<sup>3</sup> C-H oxidation via Cu-based enzyme mimetic catalysis with excellent site- and enantioselectivity; C-H bonds with similar BDEs.

Since the first reports in K-S reaction in 1958<sup>22</sup>, the copper-catalyzed radical-mediated oxidation has emerged as an important method for the selective oxidation of allylic, propargylic, and other *sp*<sup>3</sup> C-H bonds,

where *tert*-butoxy radical was proposed as HAA species<sup>23-25</sup>. Since 1995, many efforts over the last several decades have been made to develop enantioselective K-S reactions (Fig. 1C)<sup>26-29</sup>. However, most reported reactions suffered from low-to-moderate enantioselectivities and low reactivities, and a large excess of cyclic alkenes (typical 5~10 equiv.) is often required and the peroxide ester is used as the limiting reagent<sup>30</sup>, not to mention the site- and enantioselective *sp*<sup>3</sup> C-H oxidation toward substrates bearing multiple similar C-H bonds. These limitations have significantly eroded the synthetic utility over the 60-year history of the reaction.

In recent years, we have developed an efficient Cu-catalyzed radical relay strategy for the asymmetric functionalization of *sp*<sup>3</sup> C-H bonds, by which C-H substrates are employed as the limiting reagents to give C-H functionalization products in good yields, excellent site- and enantioselectivities<sup>31,32</sup>. These studies encouraged us to survey site- and enantioselective *sp*<sup>3</sup> C-H oxidation. Our initial study was commenced from the asymmetric allylic C-H oxidation of classic cyclic substrate **1a**; as mentioned above, the reaction efficiency with one equivalent of substrate presents a long-standing challenge in the field. Employing Cu(I)/Box (bisoxazoline) as the catalyst and *tert*-butyl peroxy-benzoate **2a** as the source of *tert*-butoxy radical, the reaction of **1a** with various Box ligands showed poor reactivities in acetonitrile, which is consistent with the literature reports. For instance, the reaction with Box **L2** and (CuOTf)<sub>2</sub> • toluene as the catalyst gave product **3a** in low yield (< 20% yield), *albeit* with a moderate enantiomeric ratio (87.5:12.5 er, Fig. 2A, left). Further solvent screening revealed that, fluorinated alcohols (e.g., CF<sub>3</sub>CH<sub>2</sub>OH) gave a pleasant surprise for the asymmetric C-H oxidation reaction: the yield was dramatically increased to 74%, and the enantiomeric ratio of product **3a** was also improved to 92:5:7.5. Under CF<sub>3</sub>CH<sub>2</sub>OH-based conditions, the literature reported ligand **L1** gave a slightly low yield (60%) and enantiomeric ratio (88:12). Similar results were also obtained in the reactions of cyclohexene **1b** and cycloheptene **1c**, in which the reaction efficiency was remarkably increased in CF<sub>3</sub>CH<sub>2</sub>OH (TFE) to provide products **3b-3c** in good yields

and enantioselectivities (Fig. 2A; for more optimizing reaction conditions, see the Supplementary Materials).

Encouraged by these outcomes, we further surveyed the site- and enantioselective C-H oxidation of alkene substrates with multiple sets of allylic C-H bonds. We were delighted to find that asymmetric allylic C-H oxidation of acyclic alkenes was also achieved under CF<sub>3</sub>CH<sub>2</sub>OH-solvated, copper-based catalytic

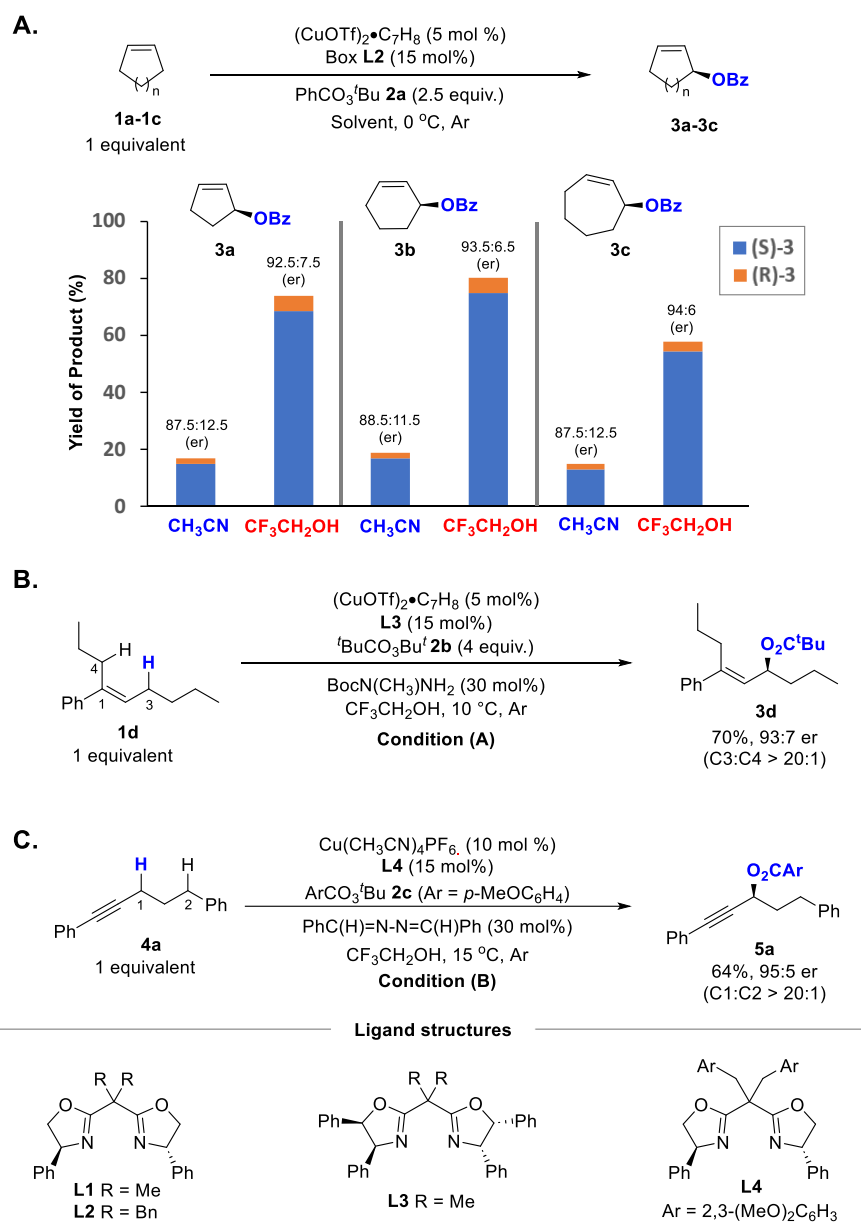


**Fig. 2. Initial results on the enantioselective sp<sup>3</sup> C-H oxidation with C-H substrates as the limiting reagents. A.** Asymmetric allylic C-H oxidation of cyclic alkenes. **B.** Site- and enantioselective allylic C-H oxidation of alkenes with two sets of allylic C-H bonds. **C.** asymmetric propargylic C-H oxidation of alkynes. Isolated yield is provided for a 0.2 mmol scale reaction, and the site-selectivity was measured for the crude product by <sup>1</sup>H NMR spectroscopy.

system, where Box **L3** was used as the ligand and peroxide ester **2b** was employed as the oxidant (condition A), and the reaction of **1d** exhibited excellent site- and regioselectivity to give product **3d** in 70% yield with 93:7 er, where the HAA process exclusively occurred at the C3-position. The similar catalytic system was also effective for the propargylic C-H oxidation. For the substrate **4a** bearing both propargylic and benzylic C-H bonds, the reaction occurred exclusively at the propargylic carbon (C1) to give **5a** in 64% yield with 95:5 er under condition B with **L4** as the ligand and **2c** as the oxidant. In these two cases, notably, the catalytic amount of reduction reagent (i.g., 1-Boc-1-methylhydrazine or benzaldehyde azine) was added to improve the reaction yields, which is for the regeneration of Cu(I) from inactive Cu(II) species<sup>29,33</sup>.

Since the discovery of K-S reaction, many efforts have been made for the mechanistic study, where the free *tert*-butoxy radical was generally considered as HAA acceptor<sup>34-37</sup>. However, the extraordinary high efficiency and excellent site-selectivity in CF<sub>3</sub>CH<sub>2</sub>OH promoted us to explore the possibility of the interaction between Box-Cu species and *tert*-butoxy radicals in the site-selective HAA process. To this end, the alkenyl peroxide substrate **6** was synthesized to test the tandem radical cyclization and addition reaction with radical trapping reagent **7**. To our excitement, the reaction in CF<sub>3</sub>CH<sub>2</sub>OH yielded a cyclization product **8** with 64:36 er, but a racemic product **8** was obtained when the reaction was conducted in CH<sub>3</sub>CN (Fig. 3A). In addition, the subtle difference between two propargylic C-H bonds in **4b** and **4c** was distinguishable in CF<sub>3</sub>CH<sub>2</sub>OH by tuning the steric hindrance of Box ligands: the ratio of **5b** and **5c** ranged from 1.5:1 for **L1** to 4.7:1 for **L5** (Fig. 3B). As a comparison, a 1:1 ratio was always observed for the reactions carried out in CH<sub>3</sub>CN with various ligands, which is consistent with the results in the radical C-H chlorination under reported metal-free condition (see Supplementary Material)<sup>38,39</sup>. These results suggest that Box-Cu species should be involved in the *tert*-butoxy radical-mediated radical cyclization or HAA step in CF<sub>3</sub>CH<sub>2</sub>OH, but not in CH<sub>3</sub>CN.

Furthermore, as shown in Fig. 3C, the single electron transfer (SET) reaction between peroxide ester **2c** and (**L4**)Cu(I) catalyst in CF<sub>3</sub>CH<sub>2</sub>OH is much faster than that in CH<sub>3</sub>CN. Such phenomenon was

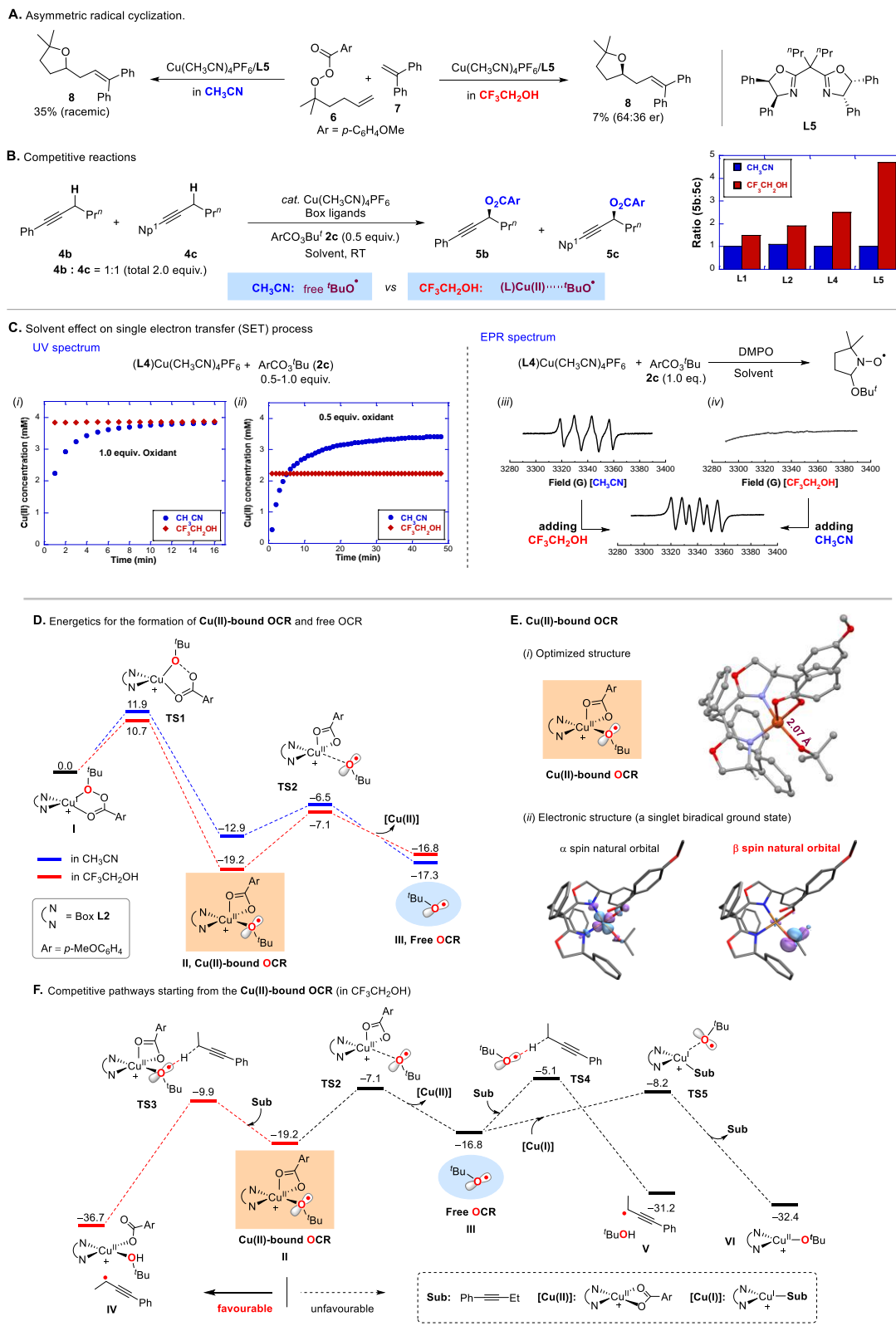


**Fig. 3. Mechanistic investigations on the reactions in CH<sub>3</sub>CN and CF<sub>3</sub>CH<sub>2</sub>OH.** **A.** Enantioselective radical cyclization. **B.** Competitive HAA experiments, Np<sup>1</sup> = 1-naphthalenyl. **C.** Studies of single electron transfer (SET) of copper catalyst and oxidant **2c**. **D.** DFT calculations, and comparison of the energetics for the formation of Cu(II)-bound OCR and free OCR in different solvents. **E.** (i) Optimized structure of Cu(II)-bound OCR, (ii) singlet biradical ground state electronic structure with spin natural orbitals that accommodate α and β electrons. **F.** Energy profiles for the competitive pathways starting from the Cu(II)-bound OCR. The box ligand **L2** and peroxide **2c** were used in the DFT calculations. Relative free energies are given in kcal/mol.

attributed to the enhanced oxidation ability of **2c** by acidic  $\text{CF}_3\text{CH}_2\text{OH}$ , which was supported by cyclic voltammetric studies (see the supplementary materials). There are two interesting observations: (1) when **2c** and the copper(I) catalyst were mixed in a 1:1 ratio, the latter was fully oxidized to a Cu(II) species in both solvents (see Fig. 3C, *i*); (2) when 0.5 equivalent of oxidant was employed, however, a nearly full conversion of copper(I) (> 90%) to Cu(II) species was observed in  $\text{CH}_3\text{CN}$ , while only half of the Cu(I) catalyst (~ 55%) was oxidized in  $\text{CF}_3\text{CH}_2\text{OH}$  (see Fig. 3c, *ii*). These observations indicated that one molecule of peroxide ester oxidizes two molecules of Cu(I) catalyst in  $\text{CH}_3\text{CN}$ , while only reacts with one molecule of Cu(I) in  $\text{CF}_3\text{CH}_2\text{OH}$ . These SET reactions were then monitored by EPR with DMPO (5,5-dimethyl-1-pyrroline N-oxide) as a radical trap. Strikingly, compared to a commonly reported organoradical species detected in  $\text{CH}_3\text{CN}$ , there was no organoradical species detected in  $\text{CF}_3\text{CH}_2\text{OH}$  (Fig. 3C, *iii-iv*). However, adding extra  $\text{CH}_3\text{CN}$  to the reaction in  $\text{CF}_3\text{CH}_2\text{OH}$  led to the appearance of EPR signals, albeit with a distinct splitting, resulting from the solvent effect<sup>40</sup>, and see the supplementary materials). The organoradical species detected in these reactions was assigned to *tert*-butoxy radical-DMPO adduct according to the literature report and our mechanistic analysis<sup>41</sup>. The discrepancy of EPR signals in different media might result from the solvent effect<sup>42</sup>.

Collectively, the observed results (Figs. 3A-B) suggested that free *tert*-butoxy radical should be involved in the catalytic reaction *in CH<sub>3</sub>CN*. The low efficiency with HAA in  $\text{CH}_3\text{CN}$  suggests that the incipient free *tert*-butoxy radical has predominately been quenched by excess Cu(I) in solution to deliver inactive Cu(II) species, leading to the termination of catalytic cycle and low catalytic efficiency (Fig. S5)<sup>43</sup>. In contrast, the outcomes observed *in CF<sub>3</sub>CH<sub>2</sub>OH* indicated that the key *tert*-butoxy radical might be coordinated to (Box)Cu(II), whereby quenching this new alkoxy radical species by Cu(I) species could be significantly alleviated or even inhibited owing to the steric hindrance (Fig. S5). Therefore, it is possible



that the Cu(II)-bound oxy-centered radical (OCR) acts as an active species *in CF<sub>3</sub>CH<sub>2</sub>OH* to undergo a HAA process, allowing for more efficient asymmetric C-H oxidation.

We further performed density functional theory (DFT) calculations, considering the propargylic C-H oxidation of 1-butynylbenzene with peroxide ester **2c** using ligand **L2**. The calculation results indicate that the rate-determining SET process starting with a copper(I) complex, which is formed between the (Box)Cu(I) fragment and **2c**, generates a crucial intermediate of Cu(II)-bound OCR (Fig. 3D). Interestingly, the Cu(II)-bound OCR exhibits significantly different kinetic and thermodynamic stability in the two solvents. Formation of the Cu(II)-bound OCR undergoes a lower energy barrier in CF<sub>3</sub>CH<sub>2</sub>OH than that in CH<sub>3</sub>CN, which is consistent with the experimental observations that SET occurs faster in CF<sub>3</sub>CH<sub>2</sub>OH (Fig. 3C, *i-ii*). Additionally, the Cu(II)-bound OCR is more stable than the free OCR by 2.4 kcal/mol in CF<sub>3</sub>CH<sub>2</sub>OH, but the free OCR is more stable in CH<sub>3</sub>CN. Based on the DFT findings and the experimental observations, we infer that the Cu(II)-bound OCR is more prevalent *in CF<sub>3</sub>CH<sub>2</sub>OH*, while the chemical equilibrium shifts towards the free OCR *in CH<sub>3</sub>CN*. Based on the DFT results presented in Fig. 3D, it is evident that the Cu(II)-bound OCR is more stable in the more polar solvent *CF<sub>3</sub>CH<sub>2</sub>OH*.

The Cu(II)-bound OCR adopts a square pyramidal geometry with a strong Cu-OCR coordination bond (2.07 Å) at the basal position (Fig. 3E, *i*), and its electronic structure is that of a singlet biradical. As revealed by the spin natural orbitals, there is one  $\alpha$  electron on a Cu center, which is antiferromagnetically coupled with one  $\beta$  electron on the *tert*-butoxy (Fig. 3E, *ii*). The singlet biradical ground state can account for the silent EPR signal as shown in Fig. 3C, *iv*, under which conditions the Cu(II)-bound OCR was formed. In this case, adding the coordinating solvent CH<sub>3</sub>CN into the mixture could promote the dissociation of *tert*-butoxy radical from the Cu(II) center, which could be immediately trapped by DMPO, leading to the appearance of the EPR signal.

Subsequently, the reactivity of Cu(II)-bound OCR in CF<sub>3</sub>CH<sub>2</sub>OH was calculated (Fig. 3F). Compared to its dissociation pathway ( $\Delta G^\ddagger = 12.1$  kcal/mol), Cu(II)-bound *tert*-butoxy radical abstracting a

propargylic hydrogen atom exhibits a lower energy barrier ( $\Delta G^\ddagger = 9.3$  kcal/mol), resulting in the favorable C-H oxidation. It should be noted that *the energy barrier of HAA process with Cu(II)-OCR ( $\Delta G^\ddagger = 9.3$  kcal/mol) is obviously lower than that of free OCR ( $\Delta G^\ddagger = 11.8$  kcal/mol)*, which is possibly attributed to the strong coordination between oxygen and copper in Cu(II)-bound OCR species. This result is further supported by competitive kinetic isotopic effect experiments, in which a relatively smaller KIE value (2.5) was observed for the reaction in CF<sub>3</sub>CH<sub>2</sub>OH, while a higher value (4.2) was observed in CH<sub>3</sub>CN (see Fig. S8 in the Supplementary Materials), suggesting that the Cu(II)-bound OCR exhibits a stronger HAA ability than the free *tert*-butoxy radical<sup>44</sup>. Furthermore, compared to the HAA process ( $\Delta G^\ddagger = 11.8$  kcal/mol), free *tert*-butoxy radical exhibits a lower energy barrier toward trapping by Cu(I) species ( $\Delta G^\ddagger = 8.7$  kcal/mol), which is consistent with the catalytic results in CH<sub>3</sub>CN (Fig 2A). In addition, directly quenching the Cu(II)-bound OCR by a Cu(I) complex seems impossible due to the steric hindrance. Sequentially, the enantioselective trapping allylic radicals by chiral BoxCu(II) species<sup>45-49</sup> was also surveyed, which supported an inner sphere pathway for the C-O bond formation (see the supplementary materials). Overall, the Cu(II)-bound OCR replicates the main structural features present at the enzyme active sites of LPMO and pMMO, especially the copper-bound, alkoxy radical that is critical for efficient and selective C(*sp*<sup>3</sup>)-H oxidation.

With the established reaction conditions in hand, the substrate scope of alkenes was initially surveyed for the asymmetric allylic C-H oxidation under the reaction condition **A** (for details, see the Supplementary Materials). As shown in Fig. 4A, a wide range of aryl-substituted alkenes with different alkyl chains were suitable substrates to deliver the corresponding chiral allylic esters **3e-3j** in good yields (51-70%) and excellent enantiomeric ratio (up to 97.5:2.5 er). The allylic C-H oxidation reaction shows a broad scope on aryl-substituted alkenes, where a series of functional groups (e.g., halide, imides, ester, *etc.*) either on the aryl ring or carbon chain are well tolerated (For more examples, see the Supplementary Materials). Moreover, heteroaryl group (e.g., thiophene, **3k**) was also tolerated. Notably, silyl-substituted alkene (**3l**)

and allylic ester (**3m**) were suitable for the allylic C-H oxidation with acceptable reaction efficiency and good to excellent enantioselectivities. To probe the site-selective C-H functionalization, we turned our attention to the alkene substrates bearing two or more sets of allylic C-H bonds. Similar to substrate **1d** (Fig. 2B), the reactions exhibited excellent performance on the site- (typically > 20:1) and enantioselective control (up to 96.5:3.5 er), where the HAA process occurred exclusively at the less sterically bulky allylic position (e.g., **3d**, **3p-3u**), or relatively weak allylic C-H bonds (e.g., **3q**). For the substrates bearing both allylic and benzylic C-H bonds, the reaction occurred exclusively at the allylic position (**3n-3o**), even for substrates bearing tertiary benzylic C-H bonds (e.g., **3o**). Notably, substrates containing piperidine moiety (**3u**) and (1*S*)- $\beta$ -pinene (**3v**) were suitable for the reaction to introduce chiral C-O bond conveniently. It is emphasized that, for the final allylic C-O bond formation, all these reactions provided excellent regioselectivity (r.r. > 20:1) and enantiomeric ratio; alkenes with both *E*- and *Z*-configurations displayed similar reactivity to yield *E*-products exclusively. Of special note, almost identical results were obtained on the gram scale (see products **3n** in 1 mmol and **3o** in 2 mmol scale).

The copper-based biomimetic catalysis reported here is also applicable for highly selective late-stage functionalization of natural products and pharmaceuticals or their derivatives. For instance, the reaction of substrates from oleanolic acid and ursolic acid provided **3w** and **3x** in 63% and 54% yields, respectively, along with excellent diastereomeric ratio (dr > 20:1). For dehydroandrosterone acetate and stigmasterol acetate containing two or four different types of allylic hydrogens, the reaction exhibited remarkably high site-, regio- and diastereoselectivity, leading to single oxidation products **3y** and **3z**, respectively. Moreover, the natural product (-)- $\alpha$ -Cedrene bearing three allylic C-H bonds was also demonstrated as a viable substrate. Its reaction predominately occurred at C1 to give natural product *sec*-cedrenol **3aa** in 55% yield with excellent diastereoselectivity via a sequential C-H oxidation and hydrolysis. It should be noted that **3aa** has the potential for the prevention and treatment of bronchialasthma, hyperlipidemia, and inflammation. In addition, for Valencene which contains both cyclic and terminal C-C double bonds with four sets of allylic hydrogens, the Cu(II)-bound *tert*-butoxy radical could exquisitely abstract allylic

hydrogen at the C1 position to yield product **3ab** with excellent results, which could be readily converted to the natural product *cis*-nootkatol via hydrolysis. In contrast, the direct oxidation of Valencene to nootkatol via enzyme catalysis generally give poor results for the selectivity or efficiency<sup>50</sup>. Moreover, in line with this reaction, natural product hyperhubein F was easily synthesized through further methylation, that exerts a notable neuroprotective activity<sup>51</sup>. For the silyl-protected Brefeldin A bearing three sets of allylic hydrogens along with abstractable hydrogens adjacent to the ether groups, the Cu(II)-bound *t*BuO radical exhibited exquisitely HAA ability to achieve excellent site-specificity and diastereoselectivity, leading to a single oxidation product **3ac** in 46% yield, along with around 32% of starting materials. Good substrate mass balance was also observed in other cases (e.g., **3w-3z**).

Beyond the allylic C-H oxidation, a similar CF<sub>3</sub>CH<sub>2</sub>OH-solvated, copper-based catalytic system is applicable to the asymmetric propargylic C-H oxidation under the slightly modified conditions B (for details, see the Supplementary Materials). As shown in Fig. 4B, the reaction shows a broad scope of alkynes, in which aryl- (**5b-5g**), silyl- (**5h-5i**) and tertiary alkyl-substituted alkynes (**5j-5k**) were suitable to deliver the corresponding chiral propargylic esters in good yields (55-73%) and excellent enantiomeric ratio (from 95:5 to 97:3 er). Notably, a reactive alkyl-iodine bond in the substrate (**5f**) could survive the catalytic conditions. More importantly, for substrates containing both benzylic and propargylic *sp*<sup>3</sup> C-H bonds, asymmetric C-H oxidation occurred exclusively at the propargylic position to give products **5l-5n** with excellent site-selectivity (> 20:1) and enantiomeric ratio (up to 95:5 er). In contrast, HAA reaction of **4m** under condition with free *tert*-butoxy radical exhibited extremely poor site-selectivity (~1:1) (see the Supplementary Materials)<sup>31</sup>. Very interestingly, although both aryl- and silyl-substituted alkynes were suitable for the reaction, when substrate (**5o**) has both types of propargylic C-H bonds, the reaction exhibited an exquisite site-selectivity, and the asymmetric C-H oxidation occurred exclusively at the propargylic C1 position of aryl-substituted alkynes. Again, for substrate bearing both allylic and propargylic C-H bonds, the reaction also provided excellent site-selectivity to give propargylic ester **5p** in

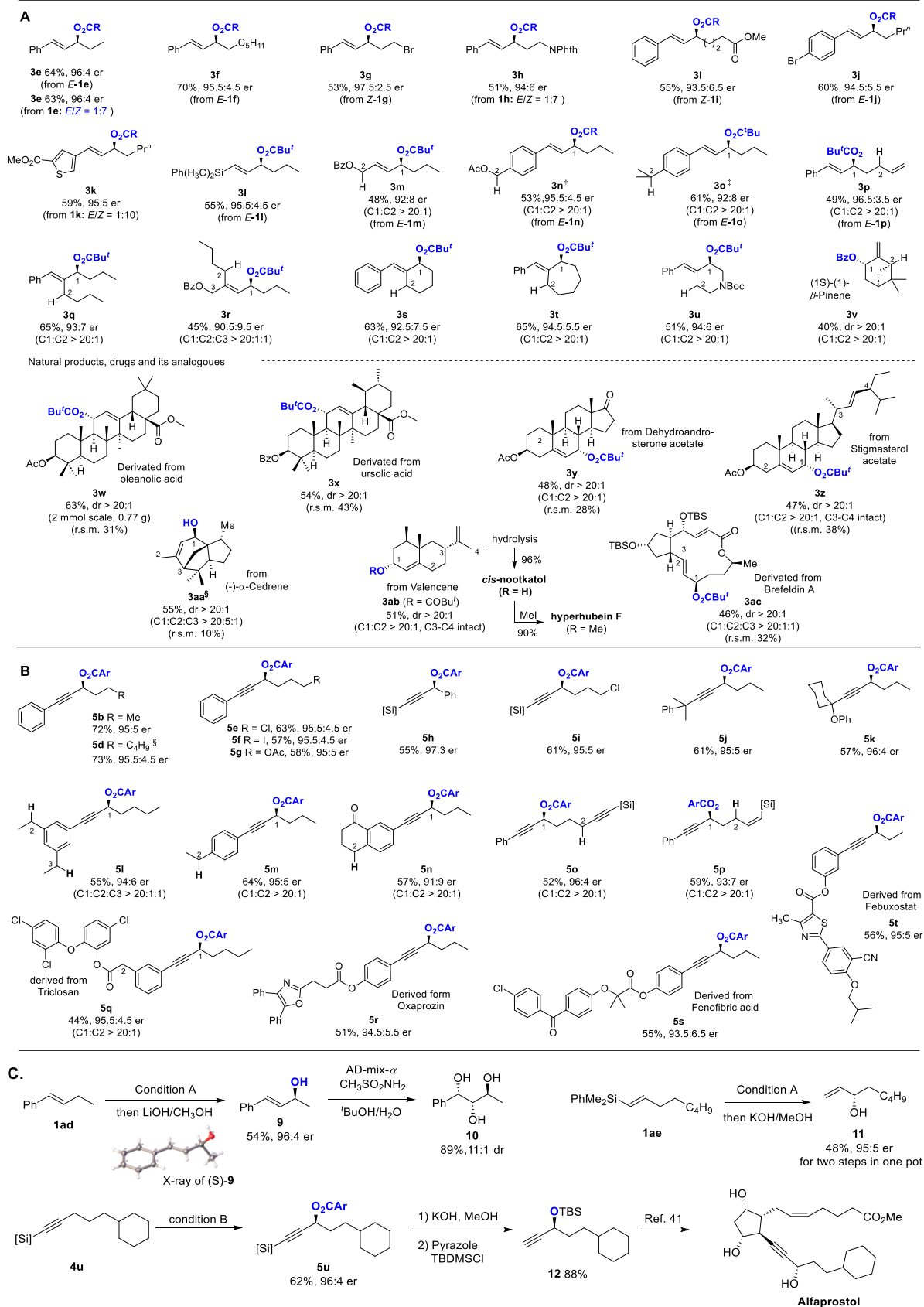


**Fig. 4. Substrate Scope on the site- and enantioselective C-H oxidation. A.** Allylic C-H oxidation of alkenes, R = C(Me<sub>2</sub>Et). **B.** Propargylic C-H oxidation of alkynes, Ar = *p*-MeOC<sub>6</sub>H<sub>4</sub>, [Si] = Si(CH<sub>3</sub>)<sub>2</sub>Ph. **C.** Synthetic application. For the detailed reaction conditions, see the Supplementary Materials; and the isolated yields were given in 0.2 mmol scale. †Reaction in 1 mmol scale. ‡Reaction in 2 mmol scale. §Sequential allylic C-H oxidation and hydrolysis. All the reactions gave excellent regioselectivity (r.r. >20:1) in the final allylic or propargylic radical C-O bond formation.

59% yield with 93:7 er. The excellent site-selectivities observed with diverse substrates provided additional evidence to support the key Cu(II)-bound *tert*-butoxy radical species for HAA, rather than free *tert*-butoxy radical.

The complex propargylic substrates derived from pharmaceuticals were also demonstrated to be good candidates for asymmetric C-H oxidation. Analogues of bioactive compounds such as triclosan (**5q**) and fenofibric acid (**5s**), analogues of drugs such as febuxostat (**5t**), and nonsteroidal *anti*-inflammatory drug oxaprozin (**5r**), can be incorporated into the alkyne substrates, which were amenable to the asymmetric propargylic C-H oxidation with good reactivities and excellent enantioselectivities.

To demonstrate the synthetic applications of the current method, as shown in Fig. 4C, allylic alcohol (*S*)-**9**, whose absolute configuration was unambiguously determined by X-ray crystallographic analysis, could also be readily synthesized from 1-phenyl-butene **1ad** via a sequential procedure with allylic C-H oxidation and hydrolysis, which can be further transformed to chiral triol **10** via dihydroxylation of alkenes in good yield and excellent diastereoselectivity (11:1). In addition, as the side chain of prostaglandin PGF<sub>2α</sub> that takes four steps from α-hydroxyketone<sup>52</sup>, the allylic alcohol **11** could be readily synthesized in 48% yield with 95:5 er, which is directly from silyl-substituted alkene **1ae** in two-steps one pot process. As mentioned above, optically pure propargylic alcohols have been recognized as valuable building blocks for the synthesis of natural products. Optically enriched propargylic ester **5u** was prepared from the corresponding alkyne **4u** in 62% yield with 96:4 er, which was readily converted to terminal propargylic silyl ether **12** in overall 88% yield with a two-steps process. This specific compound acts as a key synthon for the synthesis of nature product Alfaprostol<sup>53</sup>.

In summary, we have disclosed an unprecedented Cu(II)-bound *tert*-butoxy radical, which is crucial for the highly efficient HAA process in the case of C-H substrates used as the limiting reagents, enabling a highly efficient asymmetric allylic and propargylic C-H oxidation. The employment of fluorinated alcohols as a solvent is the key to generate Cu(II)-bound *tert*-butoxy radicals. This allows for the construction of the

necessary scaffold around copper that better mimics the active sites of enzymes involved in asymmetric C-H oxidation reactions. With the new catalytic system, our method has overcome the long-standing obstacle faced in asymmetric Kharasch-Sosnovsky reactions, including reaction efficiency, site- and enantioselectivity. The unique bind mode between radical and transition metal also laid the groundwork for further exploration of novel asymmetric C-H bond functionalization.

## References

1. Santaniello, E., Ferraboschi, P., Grisenti, P. & Manzocchi, A. The biocatalytic approach to the preparation of enantiomerically pure chiral building blocks. *Chem. Rev.* **92**, 1071-1140 (1992).
2. Noyori, R. & Ohkuma, T. Asymmetric catalysis by architectural and functional molecular engineering: practical chemo- and stereoselective hydrogenation of ketones. *Angew. Chem. Int. Ed.* **40**, 40-73 (2001).
3. Labinger, J. A. & Bercaw, J. E. Understanding and exploiting C-H bond activation. *Nature* **417**, 507-514 (2002).
4. Chakrabarty, S., Wang, Y., Perkins, J. C. & Narayan, A. R. H. Scalable biocatalytic C-H oxyfunctionalization reactions. *Chem. Soc. Rev.* **49**, 8137-8155 (2020).
5. Golden, D. L., Suh, S.-E. & Stahl, S. S. Radical C(sp<sup>3</sup>)-H functionalization and cross-coupling reactions. *Nat. Rev. Chem.* **6**, 405-427 (2022).
6. White, M. C. & Zhao, J. Aliphatic C-H oxidations for late-stage functionalization. *J. Am. Chem. Soc.* **140**, 13988-14009 (2018).
7. Che, C.-M., Lo, V. K.-Y., Zhou, C.-Y. & Huang, J.-S. Selective functionalisation of saturated C-H bonds with metalloporphyrincatalysts. *Chem. Soc. Rev.* **40**, 1950-1975 (2011).
8. Milan, M., Salamone, M., Costas, M. & Bietti, M. The quest for selectivity in hydrogen atom transfer based aliphatic C-H bond oxygenation. *Acc. Chem. Res.* **51**, 1984-1995 (2018).
9. Chen, M. S. & White, M. C. Combined effects on selectivity in Fe-catalyzed methylene oxidation. *Science* **327**, 566-571 (2010).
10. Horn, E. J., Rosen, B. R., Chen, Y., Tang, J., Chen, K., Eastgate, M. D. & Baran, P. S. Scalable and sustainable electrochemical allylic C-H oxidation. *Nature* **533**, 77-81 (2016).
11. Saint-Denis, G., Zhu, R.-Y., Chen, G., Wu, Q.-F., Yu, J.-Q. Enantioselective C(sp<sup>3</sup>)-H bond activation by chiral transition metal catalysts. *Science* **359**, eaao4798 (2018).
12. Covell, D. J., White, M. C. A Chiral Lewis Acid Strategy for Enantioselective Allylic C-H Oxidation. *Angew. Chem. Int. Ed.* **47**, 6448-6451 (2008).
13. Wang, P.-S., Liu, P., Zhai, Y.-J., Lin, H.-C., Han, Z.-Y. & Gong, L.-Z. Asymmetric allylic C-H oxidation for the synthesis of chromans. *J. Am. Chem. Soc.* **137**, 12732-12735 (2015).
14. Cianfanelli, M., Olivo, G., Milan, M., Klein Gebbink, R. J. M., Ribas, X., Bietti, M. Costas, M. Enantioselective C-H lactonization of unactivated methylenes directed by carboxylic acids. *J. Am. Chem. Soc.* **142**, 1584-1593 (2020).
15. Nie, X., Ye, C.-X., Ivlev, S.-I. & Meggers, E. Nitrene-mediated C-H oxygenation: catalytic enantioselective formation of five-membered cyclic organic carbonates. *Angew. Chem. Int. Ed.* **61**, e202211971 (2022).
16. Ortiz de Montellano, P. R. Hydrocarbon hydroxylation by cytochrome P450 enzymes. *Chem. Rev.* **110**, 932-948 (2010).
17. Ciano, L., Davies, G. J., Tolman, W. B. & Walton, P. H. Bracing copper for the catalytic oxidation of C-H bonds. *Nat. Catal.* **1**, 571-577 (2018).

18. Wang, V. C. C., Maji, S., Chen, P. P.-Y., Lee, H. K., Yu, S. S.-F. & Chan, S. I. Alkane oxidation: methane monooxygenases, related enzymes, and their biomimetics. *Chem. Rev.* **117**, 8574-8621 (2017).
19. Lieberman, R. L. & Rosenzweig, A. C. Crystal structure of a membrane bound metalloenzyme that catalyses the biological oxidation of methane. *Nature* **434**, 177-182 (2005).
20. Balasubramanian, R. et al. Oxidation of methane by a biological dicopper centre. *Nature* **465**, 115-119 (2010).
21. Elwell, C. E., Gagnon, N. L., Neisen, B. D., Dhar, D., Spaeth, A. D., Yee, G. M. & Tolman, W. B. Copper-oxygen complexes revisited: structures, spectroscopy, and reactivity. *Chem. Rev.* **117**, 2059-2107 (2017).
22. Kharasch, M. S. & Sosnovsky, G. The Reactions of *t*-butyl perbenzoate and olefins—a stereospecific reaction. *J. Am. Chem. Soc.* **80**, 756 (1958).
23. Kropf, H., Schröer, R. & Fösing, R. Kharasch-Sosnovsky-Reaktionen von Alkylen und Tetramethylen. *Synthesis* 894-896 (1977).
24. Tran, B. L., Driess, M. & Hartwig, J. F. Copper-catalyzed oxidative dehydrogenative carboxylation of unactivated alkanes to allylic esters via alkenes. *J. Am. Chem. Soc.* **136**, 17292-17301 (2014).
25. Golden, D. L., Zhang, C., Chen, S.-J., Vasilopoulos, A., Guzei, I. A. & Stahl, S. S. Benzylic C-H esterification with limiting C-H substrate enabled by photochemical redox buffering of the Cu catalyst. *J. Am. Chem. Soc.* **145**, 9434-9440 (2023).
26. Eames, J. & Watkinson, M. Catalytic allylic oxidation of alkenes using an asymmetric Kharasch-Sosnovsky reaction. *Angew. Chem. Int. Ed.* **40**, 3567-3571 (2001).
27. Zhang, B., Zhu, S.-F. & Zhou, Q.-L. Copper-catalyzed enantioselective allylic oxidation of acyclic olefins. *Tetrahedron Lett.* **54**, 2665-2668 (2013).
28. Clark, J. S., Tolhurst, K. F., Taylor, M. & Swallow, S. Enantioselective propargylic oxidation. *Tetrahedron Lett.* **39**, 4913-4916 (1998).
29. Andrus, M. B. & Lashley, J. C. Copper catalyzed allylic oxidation with peresters. *Tetrahedron*, **58**, 845-866 (2002).
30. Andrus, M. B. & Zhou, Z. Highly enantioselective copper-bisoxazoline-catalyzed allylic oxidation of cyclic olefins with *tert*-butyl *p*-nitroperbenzoate. *J. Am. Chem. Soc.* **124**, 8806-8807 (2002).
31. Wang, F., Chen, P. & Liu, G. Copper-catalyzed radical relay for asymmetric radical transformations. *Acc. Chem. Res.* **51**, 2036-2046 (2018).
32. Li, J., Zhang, Z., Wu, L., Zhang, W., Chen, P., Lin, Z. & Liu, G. Site-specific allylic C-H bond functionalization with a copper-bound N-centred radical. *Nature* **574**, 516-521 (2019).
33. Hu, H., Chen, S.-J., Mandal, M., Pratik, S. M., Buss, J. A., Krska, S. W., Cramer, C. J. & Stahl, S. S. Copper-catalyzed benzylic C-H coupling with alcohols via radical relay enabled by redox buffering. *Nat. Catal.* **3**, 358-367 (2020).
34. Walling, C. & Zavitsas, A. A. The Copper-Catalyzed Reaction of Peresters with Hydrocarbons. *J. Am. Chem. Soc.* **85**, 2084-2090 (1963).
35. Kochi, J. K. & Mains, H. E. Studies on the Mechanism of the Reaction of Peroxides and Alkenes with Copper Salts. *J. Org. Chem.* **30**, 1862-1872 (1965).
36. Beckwith, A. L. J. & Zavitsas, A. A. Allylic oxidations by peroxy esters catalyzed by copper salts. The potential for stereoselective syntheses. *J. Am. Chem. Soc.* **108**, 8230-8234 (1986).
37. Smith, K. Hupp, C. D. Allen, K. L. & Slough, G. A. Catalytic Allylic Amination versus Allylic Oxidation: A Mechanistic Dichotomy. *Organometallics*, **24**, 1747-1755 (2005).
38. Beckwith, A. L. J. & Zavitsas, A. A. Allylic oxidations by peroxy esters catalyzed by copper Salts. The potential for stereoselective syntheses. *J. Am. Chem. Soc.* **108**, 8230-8234 (1986).
39. Quinn, R. K., Könst, Z. A., Michalak, S. E., Schmidt, Y., Szklarski, A. R., Flores, A. R., Horne, S. Nam, D. A., Vanderwal, C. D. & Alexanian, E. J. Site-selective aliphatic C-H chlorination using *N*-chloroamides enables a synthesis of chlorolissoclimide. *J. Am. Chem. Soc.* **138**, 696-702 (2016).



40. Bors, W., Michel, C. & Stettmaier, K. Solvent effects on the nitrogen and  $\beta$ -hydrogen hyperfine splitting constants of aminoxyl radicals obtained in spin trapping experiments. *J. Chem. Soc. Perkin Trans. 2*, 1513-1517 (1992).
41. Janzen, E. G., Coulter, G. A., Oehler, U. M. & Bergsma, J. P. Radical species produced from the photolytic and pulse-radiolytic degradation of *tert*-butyl hydroperoxide. An EPR spin trapping investigation. *Can. J. Chem.* **60**, 2725-2733 (1982).
42. Bors, W., Michel, C. & Stettmaier, K. Solvent effects on the nitrogen and  $\beta$ -hydrogen hyperfine splitting constants of aminoxyl radicals obtained in spin trapping experiments. *J. Chem. Soc. Perkin Trans. 2*, 1513-1517 (1992).
43. Gephart III, R. T., McMullin, C. L., Sapiezynski, N. G., Jang, E. S., Aguila, M. J. B., Cundari, T. R., & Warren, T. H. Reaction of  $\text{Cu}^{\text{I}}$  with dialkyl peroxides:  $\text{Cu}^{\text{II}}$ -alkoxides, alkoxy radicals, and catalytic C-H etherification. *J. Am. Chem. Soc.* **134**, 17350-17353 (2012).
44. An, Q., Xing, Y.-Y., Pu, R., Jia, M., Jia, Y., Chen, Y., Hu, A., Zhang, S.-Q., Yu, N., Du, J., Zhang, Y., Chen, J., Liu, W., Hong, X. & Zuo, Z. Identification of alkoxy radicals as hydrogen atom transfer agents in Ce-catalyzed C-H functionalization. *J. Am. Chem. Soc.* **145**, 359-376 (2023).
45. Fan, L.-F., Liu, R., Ruan, X.-Y., Wang, P.-S. & Gong, L.-Z. Asymmetric 1,2-oxidative alkylation of conjugated dienes via aliphatic C-H bond activation. *Nat. Synth.* **1**, 946-955 (2022).
46. Chen, J., Liang, Y.-J., Wang, P.-Z., Li, G.-Q., Zhang, B., Qian, H., Huan, X.-D., Guan, W., Xiao, W.-J. & Chen, J.-R. Photoinduced copper-catalyzed asymmetric C-O cross-coupling. *J. Am. Chem. Soc.* **143**, 13382-13392 (2021).
47. Wang, P.-Z., Wu, X., Cheng Y., Jiang, M., Xiao, W.-J. & Chen, J.-R. Photoinduced copper-catalyzed asymmetric three-component coupling of 1,3-dienes: an alternative to Kharasch-Sosnovsky reaction. *Angew. Chem. Int. Ed.* **60**, 22956-22962 (2021).
48. Zhu, X., Jian, W., Huang, M., Li, D., Li, Y., Zhang, X. & Bao, H. Asymmetric radical carboesterification of dienes. *Nat. Commun.* **12**, 6670 (2021).
49. Nie, Z., Chiou, M.-F., Cui, J., Qu, Y., Zhu, X., Jian, W., Xiong, H., Li, Y. & Bao, H. Copper-catalyzed radical enantioselective carbo-esterification of styrenes enabled by a perfluoroalkylated-PyBox ligand. *Angew. Chem. Int. Ed.* **61**, e202202077 (2022).
50. Sowden, R. J., Yasmin, S., Rees, N. H., Bell, S. G. & Wong, L.-L. Biotransformation of the sesquiterpene (+)-valencene by cytochrome P450<sub>cam</sub> and P450<sub>BM-3</sub>. *Org. Biomol. Chem.* **3**, 57-64 (2005).
51. Yan, X.-T., Chen, J.-X., Wang, Z.-X., Zhang, R.-Q., Xie, J.-Y., Kou, R.-W., Zhou, H.-F., Zhang, A.-L., Wang, M.-C., Ding, Y.-X. & Gao, J.-M. Hyperhubeins A-I, Bioactive sesquiterpenes with diverse skeletons from hypericum hubeiense. *J. Nat. Prod.* **86**, 119-130 (2023).
52. Zhang, F., Zeng, J., Gao, M., Wang, L., Chen, G.-Q., Lu, Y. & Zhang, X. Concise, scalable and enantioselective total synthesis of prostaglandins. *Nat. Chem.* **13**, 692-697 (2021).
53. Baars, H., Classen, M. J. & Aggarwal, V. K. Synthesis of Alfaprostol and PGF<sub>2 $\alpha$</sub>  through 1,4-Addition of an Alkyne to an Enal Intermediate as the Key Step. *Org. Lett.* **19**, 6008-6011 (2017).

## Acknowledgments

Financial Support was provided by the National Key R&D Program of China (Grant 2021YFA1500100), the National Nature Science Foundation of China (Grants 22331012, 91956202, 92256301, and 21821002), the Science and Technology Commission of Shanghai Municipality (Grants 20JC1417000, and 21520780100), and the International Partnership Program (Grant 121731KYS-B20190016) of the Chinese Academy of Sciences, and the Research Grants Council of Hong Kong (HKUST 16300620 and 16302222). H.Z. thanks Dr. Yanxia Zhang for the EPR manipulation and analysis. G.L. acknowledges support from the Tencent Foundation through the New Cornerstone Science Foundation

**Author Contributions** HZ, YZ, JW and GL conceived the work and designed the experiments. HZ, YZ performed the predominated laboratory experiments, and JW contributed partly. TY and ZL conducted DFT calculation. HZ, YZ, PC and GL analysed the data and wrote the manuscript.